



## Research article

# Air pollution nanoparticle and alpha-synuclein fibrils synergistically decrease glutamate receptor A1, depending upon nPM batch activity



Hongqiao Zhang<sup>a,\*</sup>, Carla D'Agostino<sup>a</sup>, Christopher Tulisiak<sup>b,1</sup>, Max A. Thorwald<sup>a</sup>, Liza Bergkvist<sup>b</sup>, Allison Lindquist<sup>b</sup>, Lindsay Meyerdirk<sup>b</sup>, Emily Schulz<sup>b</sup>, Katelyn Becker<sup>b</sup>, Jennifer A. Steiner<sup>b</sup>, Mafalda Cacciottolo<sup>a,2</sup>, Mohit Kwatra<sup>b</sup>, Nolwen L. Rey<sup>b,3</sup>, Martha L. Escobar Galvis<sup>b</sup>, Jiyan Ma<sup>b,4</sup>, Constantinos Sioutas<sup>c</sup>, Todd E. Morgan<sup>a</sup>, Caleb E. Finch<sup>a</sup>, Patrik Brundin<sup>b,5</sup>

<sup>a</sup> Leonard Davis School of Gerontology, University of Southern California, USA

<sup>b</sup> Van Andel Institute, Grand Rapids, MI 49503, USA

<sup>c</sup> Viterbi School of Engineering, University of Southern California, Los Angeles, CA 90089, USA

## ARTICLE INFO

## Keywords:

Parkinson's disease  
α-synuclein  
Air pollution  
Nanoparticles  
Iba1  
Glutamate receptor A1

## ABSTRACT

**Background:** Epidemiological studies have variably linked air pollution to increased risk of Parkinson's disease (PD). However, there is little experimental evidence for this association. Alpha-synuclein (α-syn) propagation plays central roles in PD and glutamate receptor A1 (GluA1) is involved in memory and olfaction function.

**Methods:** Each mouse was exposed to one of three different batches of nano-particulate matter (nPM) (300 μg/m<sup>3</sup>, 5 h/d, 3 d/week), collected at different dates, 2017–2019, in the same urban site. After these experiments, these nPM batches were found to vary in activity. C57BL/6 female mice (3 mo) were injected with pre-formed murine α-synuclein fibrils (PFFs) (0.4 μg), which act as seeds for α-syn aggregation. Two exposure paradigms were used: in Paradigm 1, PFFs were injected into olfactory bulb (OB) prior to 4-week nPM (Batch 5b) exposure and in Paradigm 2, PFFs were injected at 4th week during 10-week nPM exposure (Batches 7 and 9). α-syn pSer129, microglia Iba1, inflammatory cytokines, and *Gria1* expression were measured by immunohistochemistry or qPCR assays.

**Results:** As expected, α-syn pSer129 was detected in ipsilateral OB, anterior olfactory nucleus, amygdala and piriform cortex. One of the three batches of nPM caused a trend for elevated α-syn pSer129 in Paradigm 1, but two other batches showed no effect in Paradigm 2. However, the combination of nPM and PFF significantly decreased *Gria1* mRNA in both the ipsi- and contralateral OB and frontal cortex for the most active two nPM batches. Neither nPM nor PFFs alone induced responses of microglia Iba1 and expression of *Gria1* in the OB and cortex.

\* Corresponding author.

E-mail address: [hongqiaz@usc.edu](mailto:hongqiaz@usc.edu) (H. Zhang).

<sup>1</sup> Current employer: Meso-Scale Discovery, Rockville, MD, USA

<sup>2</sup> Current employer: Capricor Therapeutics, Inc., San Diego, CA, USA

<sup>3</sup> Current employer: UMR9199 CNRS-CEA, MIRCen, Fontenay-aux-Roses, France.

<sup>4</sup> Current institution: Chinese Institute for Brain Research, Beijing, China.

<sup>5</sup> Current employer: F. Hoffmann-La Roche, Basel, Switzerland.

<https://doi.org/10.1016/j.heliyon.2023.e15622>

Received 4 November 2022; Received in revised form 3 April 2023; Accepted 17 April 2023

Available online 19 April 2023

2405-8440/© 2023 The Authors. Published by Elsevier Ltd. This is an open access article under the CC BY-NC-ND license (<http://creativecommons.org/licenses/by-nc-nd/4.0/>).

**Conclusion:** Exposures to ambient nPM had weak effect on  $\alpha$ -syn propagation in the brain in current experimental paradigms; however, nPM and  $\alpha$ -syn synergistically downregulated the expression of *Gria1* in both OB and cortex.

## 1. Introduction

Parkinson's disease (PD) is one of the most common neurodegenerative disorders, affecting 1% of 60 years of age and older. Clinically, PD is characterized by tremor, slow movement, and rigidity; it is also associated with non-motor symptoms such as hyposmia, dementia, depression and sleep disorders, some of which may precede the motor symptoms. The hallmarks of PD pathology include accumulation of misfolded  $\alpha$ -synuclein ( $\alpha$ -syn) in Lewy bodies and Lewy neurites, and loss of dopaminergic neurons in the substantia nigra (SN). A potential molecular mechanism involves the aggregation of  $\alpha$ -syn and its *trans*-synaptic propagation to neighboring neurons where it triggers further  $\alpha$ -syn aggregation, and following axonal transport, leads to propagation of pathology between brain regions. It has been suggested that the  $\alpha$ -syn aggregates disrupt synaptic signaling and impair vital subcellular processes, e.g. in mitochondria endoplasmic reticulum and the lysosomal autophagy system [1]. Pathological  $\alpha$ -syn aggregates are postulated to arise in the olfactory bulb (OB) [2] or gut [3], and progressively propagate to the SN in a spatially stereotypic pattern, with subsequent damage to dopaminergic neurons [4]. Neuroinflammation also mediates PD pathogenesis, through pathways including promoting  $\alpha$ -syn pathology [5].

Genetic and environmental factors contribute to PD pathogenesis. Only a small proportion of PD cases are familial, and the total contribution of genetics to PD risk has been estimated to be in the range of 25% [6]. A variety of environmental toxins, e.g. 1-methyl-4-phenyl-1,2,3,6-tetrahydropyridine (MPTP), rotenone (a pesticide), paraquat (a herbicide), and heavy metals are implicated in sporadic PD [7]. Many epidemiological studies have associated air pollution exposure with PD [8–17]. Exposure to NO<sub>2</sub> [8,12,15–17], O<sub>3</sub> [10,16] and particulate matter (PM) [9,10,13,16,17] increased PD prevalence and/or incidence. In a 12-year prospective study of 2 million subjects, each interquartile increment (3.8  $\mu\text{g}/\text{m}^3$ ) of PM<sub>2.5</sub> was associated with a 4% increase in PD incidence [16]. In addition, environmental nanoparticles were detected in several brain regions including SN of urban young adult residents [18]. Moreover, animal studies show that ambient PM, especially nano-sized PM (nPM, aerodynamic diameter <0.2  $\mu\text{m}$  or PM<sub>0.2</sub>), can induce neuroinflammation [19] and increase  $\alpha$ -syn expression [20]. These findings suggest potential mechanisms for associations of ambient PM with PD. However, one conflicting report did not find association of PD with ambient PM<sub>10</sub>, PM<sub>2.5</sub> or NO<sub>2</sub> [13].

Urban ambient particles arise from diverse sources and consist of a heterogeneous mixture of sizes and chemical composition [21, 22]. This diversity of composition results in variable toxic potency for ambient particles collected at different times and sites, as demonstrated by several groups using *in vitro* cell-based NF- $\kappa$ B activity assay and test-tube-based dithiothreitol assay (oxidative potential assay) [23–27]. Recent studies from this lab showed variable neurotoxicity for nPM batches collected at same site but at different dates [28].

Experimental evidence is needed to show how air pollution may influence the progression of  $\alpha$ -syn pathology. We used a mouse model of progressive  $\alpha$ -syn neuropathology [29–36] to evaluate the effects of ambient nPM exposure on (i) levels and spread of  $\alpha$ -syn aggregates from the OB to interconnected brain regions, (ii) microglial activation and (iii) expression of glutamate receptor A1 (GluA1, encoded by *Gria1*), which is involved in learning and memory [37] and odor/olfaction memory process [38], which are relevant to PD symptoms of dementia and hyposmia. The nPM batches were collected at the same site in downtown Los Angeles, and were later shown to vary widely in activities as evaluated by induction of NF- $\kappa$ B *in vitro* and neurotoxic responses *in vivo* [28].

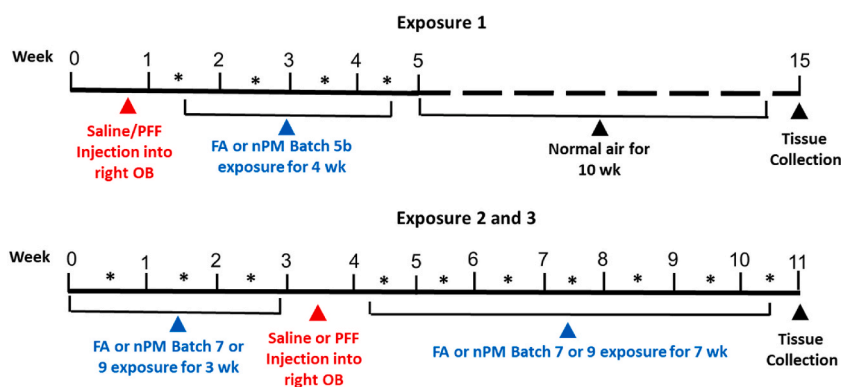


**Fig. 1.** Paradigms for PFF injection and nPM exposure. Female mice (3-mo-old) were injected with PBS or PFFs in the right OB under anesthesia. Three nPM batches were collected at different dates. Exposure 1, Batch 5b; Exposure 2, Batch 7; Exposure 3, Batch 9 (see Methods).

## 2. Methods and materials

### 2.1. Chemicals and reagents

TRIzol reagent (#15596026) was purchased from Thermal Fisher Scientific (Rockford, IL, USA); qScript cDNA superMix (#101414-108) was from Qantabio (Beverly, MA, USA); qPCR master mixture (#QPCR-10) was obtained from BioPioneer Inc. (San Diego, CA, USA); the primary antibodies for Iba1 were from FUJIFILM Wako Chemicals (#019-19741, Richmond, VA, USA) and  $\alpha$ -syn pSer129 from Abcam (#Ab51253, Cambridge, MA, USA); secondary antibodies were from Vector Laboratories Inc. (Newark, CA, USA); other reagents were from Sigma-Aldrich (St. Louis, MO, USA).

### 2.2. Animals

All animal procedures were pre-approved by the University of Southern California (USC) Institutional Animal Care and Use Committee (IACUC) and the Animal Care Use and Review Office (ACURO). Three-month-old C57BL/6NJ female mice from Jackson Laboratories were acclimated 1 week before experiments. Two experiment paradigms were examined (Fig. 1) to simulate conditions of 1) the onset of  $\alpha$ -syn pathology occurs before exposure to nPM (Paradigm 1); and 2) the onset of  $\alpha$ -syn pathology occurs during nPM exposure (Paradigm 2). Power analysis showed that at least 8 mice per group were needed to detect the effect of nPM, as used in prior studies [39,40]. Since  $\alpha$ -syn assay needed an independent set of brain samples, the size of each group was doubled ( $2 \times 8$  for Exposure 1 and  $2 \times 11$  for Exposures 2&3) for  $\alpha$ -syn and other assays. In exposure 1 (Paradigm 1), mice (64 mice, 16 mice per group) were injected with either saline (PBS) or pre-formed murine  $\alpha$ -synuclein fibrils (PFFs) and then exposed to either filtered air (FA) or nPM for 4 weeks, followed by 10 weeks of normal housing conditions before being euthanized. For Exposure 2 and 3 (Paradigm 2), mice (88 mice, 22 mice per group) were exposed to FA or nPM for 3 weeks before PFFs injection, and then continuously exposed to nPM for 7 more weeks before euthanasia. Half of the mice per group were anesthetized with isoflurane and perfused transcardially with 4% paraformaldehyde in 0.1 M phosphate buffer; brains were post-fixed, cryoprotected and sectioned for immunohistochemistry assays of  $\alpha$ -syn pSer129 and Iba1. Half of the mice were perfused with saline, and the brains were hemisected (collected as ipsilateral and contralateral, relative to the PFF injection site); the olfactory bulbs were collected, and the cortical shells were halved for collection as frontal and posterior; dissected tissues were immediately frozen on dry ice for mRNA assays.

### 2.3. nPM exposure

The 3 batches of nPM used in this study were collected at the same site within 150 m downwind of the urban freeway (I-110, Los Angeles, CA, USA) [41]. The collection dates were: Batch 5b, 2017 Oct–Dec; Batch 7, 2018 May–Jul; and Batch 9, 2019 Sep–Nov. The preparation of nPM and exposure were as described [42]. The chemical composition of the nPM samples was quantified by mass spectrometry (SF-ICPMS) by digesting a fraction of the filter-collected nPM with mixed acids (nitric acid, hydrofluoric acid, hydrochloric acid) [43]. The organic matter was analyzed using Sievers 900 Total Organic Carbon Analyzer [44]. For each exposure, mice were transferred from home cages into sealed, parallel exposure chambers: the nPM groups were exposed to re-aerosolized nPM at  $300 \mu\text{g}/\text{m}^3$ , while the FA groups received filtered air. Exposure schedules were 5 h/d, 3 d/week, for durations as indicated in Fig. 1. Mass concentration of the re-aerosolized nPM exposure stream was gravimetrically assessed on filters in parallel to the exposure stream before and after exposures. The nebulizer maintained a similar size distribution of re-aerosolized PM<sub>0.2</sub>.

### 2.4. PFFs preparation and injections

Pre-formed murine  $\alpha$ -synuclein fibrils (PFFs) were prepared as described [45]. Briefly, recombinant mouse  $\alpha$ -synuclein ( $\alpha$ -syn) was expressed in BL21 *E. coli* and purified. For amyloid fibril assembly, purified recombinant  $\alpha$ -syn was thawed and subjected to continuous shaking at  $1000 \times \text{rpm}$  at  $37^\circ\text{C}$  in an Eppendorf Thermomixer for 7 days. Fibril morphology was confirmed by imaging using a Tecnai G2 Spirit TWIN transmission electron microscope (FEI Company) and by reading Thioflavin T (Sigma) fluorescence. PFFs were stored at  $-80^\circ\text{C}$  until use.

PFF injection was as described [29]. Briefly, PFFs were thawed and sonicated at room temperature by probe sonication. The stereotactic injections used a glass capillary attached to a  $10 \mu\text{l}$  Hamilton microsyringe, and  $0.8 \mu\text{l}$  of PFFs ( $5 \mu\text{g}/\mu\text{l}$  in sterile PBS). Under deep anesthesia, PFFs or PBS were injected unilaterally into the right olfactory bulb (OB): A/P +5.4 mm, L  $-0.75$  mm, D/V

**Table 1**  
Primer sequences for qPCR assay.

Gene	Forward (5'-3')	Reverse (5'-3')
<i>Iba1</i>	CCTGATTGGAGGTGGATGTCAC	GGCTCACGATTTCTTTTTTCC
<i>Gria1</i>	GACGAGATCAGACAACCACT	AGTGAAGAACACCAGACAC
<i>Tnfa</i>	ACCTGGCCTCTCTACCTTGT	CCCGTAGGGCGATTACAGTC
<i>Il1b</i>	CTAAAGTATGGGCTGGACTG	GGCTCTCTTTGAACAGAATG
<i>Il10</i>	AGGGCCCTTTGCTATGGTGT	TGGGGGATGACAGTAGGGGA
<i>Cd68</i>	TTCTGCTGTGAAATGCAAG	AGAGGGGCTGGTAGGTTGAT
<i>Gapdh</i>	CCAATGTGTCCTCGTGGATCT	GTTGAAGTCGACAGGACAACC

–1.00 mm, at a rate of 0.2  $\mu$ l per min.

## 2.5. Quantitative PCR assay

Total RNA was extracted from OB or frontal cortex with TRIzol reagent, followed by reverse transcription (RT) (1  $\mu$ g of total RNA, 4  $\mu$ l of qScript cDNA superMix in a total volume of 20  $\mu$ l reaction) with manufacturer's protocol. The RT samples were diluted 10 times for PCR assays. The qPCR assay was conducted in 20  $\mu$ l reaction (10  $\mu$ l of qPCR master mixture, 3  $\mu$ l of RT sample, and 0.25  $\mu$ M of primers) in a Bio-Rad CFX96C1000 touch screen real time PCR system (Bio-Rad, Hercules, CA, USA). The qPCR reaction was begun with activation at 95 °C for 5 min; then 40 cycles of 95 °C, 15 s; 63 °C, 15 s; 72 °C, 20 s; followed by melting curve detection to confirm the specificity of PCR reactions. Primer sequences (Table 1) were designed by using Primer-BLAST, based on cDNA sequences obtained from NCBI-Nucleotide data base (<https://www.ncbi.nlm.nih.gov/nucleotide/>). Oligonucleotides were synthesized by Integrated DNA Technologies (IDT, Coralville, Iowa, USA). The qPCR data is analyzed by  $2^{-\Delta\Delta CT}$  method with GAPDH as the internal control for normalization. To show the reliability and precision of this assay, the coefficient of variations for *Gria1* qPCR were listed in the Supplement (Table S1) as representative.

## 2.6. Immunohistochemistry

Fixed brain tissues were sliced into 40  $\mu$ m sections and stored in 30% sucrose prior to immunostaining. Sections were rinsed with 0.1 M PBS, incubated with 3% H<sub>2</sub>O<sub>2</sub> for 20 min to quench endogenous peroxidase activity, and blocked with normal serum for 1 h. Next, sections were incubated overnight with specific antibodies ( $\alpha$ -syn pSer129, rabbit, 1:10,000, and Iba1, 1:500). After rinsing with PBS, sections were immunostained with corresponding biotinylated secondary antibodies, rinsed, then processed with a standard peroxidase-based method with 3,3'-diaminobenzidine (DAB) (VECTASTAIN ABC & DAB kits, Vector Laboratories). Subsequently, the sections were dehydrated, mounted and cover slipped for imaging.

## 2.7. $\alpha$ -syn pathology quantification

(Exposures 1 and 2) Densitometry to quantitate  $\alpha$ -syn pSer129 was conducted as in Ref. [30]. Briefly, slides blinded by a separate investigator were assayed. Using a NIKON Eclipse Ni-U microscope (Nikon), 20 $\times$  magnification images were collected (NIKON NIS Elements AR, version 4.00.08, color Retiga Exi digital CCD camera, Q Imaging) using the same exposure time for all images. For the OB, images were captured on three sections separated by 240  $\mu$ m intervals (between Bregma +4.9 and +4 mm). Three images of the medio-lateral AON were acquired (240  $\mu$ m intervals between sections, covering the whole AON; between Bregma +3 and +2 mm). Next images were processed in ImageJ to create a background-excluding mask that redirected to the original image for analysis. The total area and the mean grey value of the area that featured  $\alpha$ -syn pSer129 immunoreactivity were measured. Then the grey value per square pixels per image ( $A.U./px^2 = \text{mean grey value} \times \text{area stained}/\text{total area assessed}$ ), and the average grey value per square pixels for each brain region of each animal were calculated.

(Exposure 3) Z-stacks of mounted  $\alpha$ -syn pSer129-stained tissue sections were captured at 20 $\times$  magnification using a whole slide scanner (Zeiss, Axioscan Z1) at a 0.22  $\mu$ m/pixel resolution. Extended depth focus (EDF) was used to collapse the z-stacks into 2D images as they were collected. Tissue thickness was set to 20  $\mu$ m, z-stacks were collected at 3  $\mu$ m intervals and the method used was Contrast. The images were exported with 85% compression as.jpeg files. The digitized images were then uploaded to Aiforia™ image processing and management platform (Aiforia Technologies, Helsinki, Finland) for analysis with deep learning convolution neural networks (CNNs) and supervised learning. A supervised, multi-layered CNN was trained on annotations from digitized  $\alpha$ -syn pSer129-stained coronal slices to recognize total  $\alpha$ -syn pSer129-positive staining. The algorithm was trained on the most diverse and representative images from across multiple  $\alpha$ -syn pSer129 datasets to create a generalizable AI model that accurately detects  $\alpha$ -syn pSer129-stained profiles in slides collected by multiple investigators. Ninety-one images constituted training data. Features of interest used to train the AI model were annotated for each layer within the Aiforia™ Cloud platform and constituted input data for each CNN. The first feature layer was annotated using semantic segmentation to distinguish total tissue from the glass slide. The second feature layer was annotated using semantic segmentation to distinguish total  $\alpha$ -syn pSer129-positive staining. Features that were considered artifact (glass slide, debris) were annotated as background and constituted additional input training data for the multi-layered CNN. The regions corresponding to the AON and the piriform cortex were outlined according to the Allen Mouse Brain Atlas (Allen Institute); the CNN was used to quantify the percentage of target brain region area containing  $\alpha$ -syn pSer129-positive signal.

## 2.8. Iba1 quantitation

The density of Iba1-positive cells was quantified using NIS Elements AR 4.00.08 software (Nikon) in a blinded manner as reported [46]. Briefly, multiple fields of Iba1-positive cells were captured on a Nikon Eclipse Ni-U microscope; images were obtained with a color Retiga Exidigital CCD camera (QImaging) using NIS Elements AR 4.00.08 software (Nikon) and 20 $\times$  magnification (air immersion, 0.75 N.A., n = 3/animal/hemisphere), and the region of interest was outlined. All the Iba1-positive cells in the field of view that were within the border were counted using the count feature of the NIS Elements AR 4.00.08 software.

## 2.9. Statistical analysis

Data were analyzed by GraphPad Prism (Version 9). Statistical comparisons used Student's t-test for two groups and two-way ANOVA for 4 groups with Tukey's multiple comparisons test. The data are shown as mean  $\pm$  standard error of the mean (s.e.m) and  $P < 0.05$  is considered significant for all statistical tests.

## 3. Results

Three batches of nPM were sequentially evaluated for their impact on PFFs propagation and neurotoxicity using 2 different experimental paradigms (Fig. 1). The differences in nPM batch activity were not known until completion of these studies. Fig. 2 shows the chemical profiles of the 3 batches of nPM. These batches had similar concentrations of transition metals (Fig. 2A) but varied in other chemical composition (Fig. 2B). Notably, these three nPM batches differed in potency: Batch 9 was 3-fold more active than Batch 7 to induce *in vitro* NF $\kappa$ B response [28], though the relative *in vitro* activity of Batch 5b (Exposure 1) was not measured because the sample was depleted.

### 3.1. Exposure 1: PFFs injection prior to nPM exposure

#### 3.1.1. Effect on $\alpha$ -syn spread

Prior studies from the Brundin lab document that animals injected with PFFs in OB develop fibrillar  $\alpha$ -syn pathology in the OB, anterior olfactory nucleus (AON), and amygdala (AMY) [29,30]. In the present study, 15 weeks after PFFs injection,  $\alpha$ -syn pSer129 in the ipsilateral OB, AON, and AMY was elevated by 12-, 1310-, and 170-fold, respectively above controls injected with PBS (Fig. 3A–C). In contrast, PFFs injection did not generally increase the  $\alpha$ -syn pSer129 in the contralateral regions, except for one region, the AON, in which  $\alpha$ -syn pSer129 was increased by 180-fold above the contralateral AON of the PBS control (Fig. 3B).

Exposure to nPM (Batch 5b, Fig. 3A–C) was associated with a non-significant trend for increased  $\alpha$ -syn pSer129 in the ipsilateral OB (ipsilateral:  $22.5 \pm 19.9$  vs  $33.2 \pm 22.5$ ,  $P = 0.57$ ,  $N = 7$ ; contralateral:  $1.8 \pm 1.4$  vs  $3.1 \pm 3.5$ ,  $P = 0.94$ ,  $N = 7$ ), AON (ipsilateral:  $1219 \pm 916$  vs  $1876 \pm 853$ ,  $P = 0.25$ ,  $N = 6$ ; contralateral:  $268 \pm 237$  vs  $326 \pm 209$ ,  $P = 0.92$ ,  $N = 6$ ), and AMY (ipsilateral:  $81.8 \pm 60.1$  vs  $120 \pm 59.8$ ,  $P = 0.51$ ,  $N = 8$ ; contralateral:  $4.0 \pm 5.6$  vs  $8.3 \pm 9.1$ ,  $P = 0.44$ ,  $N = 8$ ) of the PFF groups; however, nPM alone did not alter  $\alpha$ -syn pSer129 in any examined region.

#### 3.1.2. Effect on microglia Iba1 response

We next examined this exposure to Batch 5b for effects on microglial responses to PFFs. Iba1 mRNA did not differ in the ipsilateral OB and frontal cortex (CX) between groups of PFFs (PFF + FA,  $98.8 \pm 20.0$ ,  $P = 0.99$ ,  $N = 7$  for OB,  $117 \pm 13.9$ ,  $P = 0.89$ ,  $N = 7$  for CX), nPM (PBS + nPM,  $92.1 \pm 9.9$ ,  $P = 0.93$ ,  $N = 7$  for OB,  $109 \pm 15.4$ ,  $P = 0.95$ ,  $N = 7$  for CX), PFF + nPM ( $109 \pm 9.8$ ,  $P = 0.97$ ,  $N = 7$  for OB,  $117 \pm 17.1$ ,  $P = 0.91$ ,  $N = 7$  for CX) and control group (PBS + FA,  $99.9 \pm 11.9$  for OB,  $100 \pm 13.1$  for CX) (Supplemental Fig. S1A).

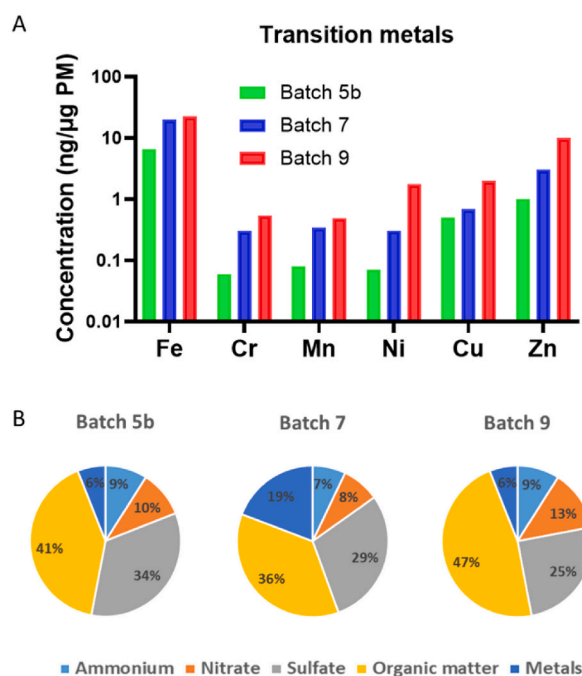
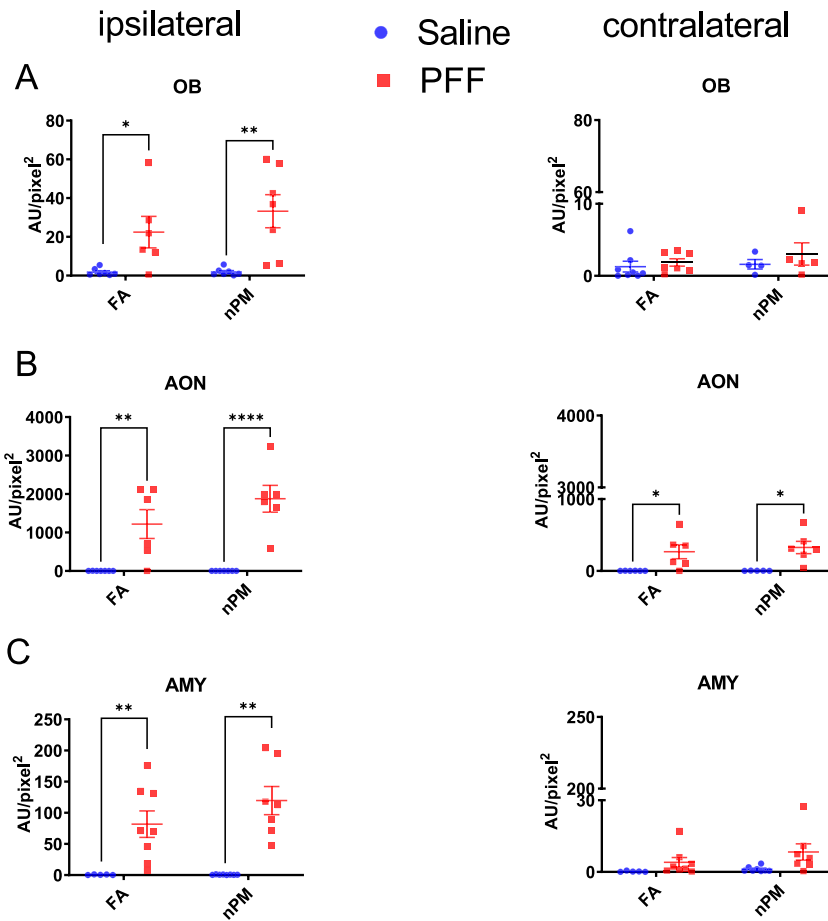


Fig. 2. Chemical composition of nPM batches. A, Transition metal concentration; B) Percentage of chemical components in total nPM mass.

### $\alpha$ -Syn pSer129



**Fig. 3.** Exposure 1 (nPM Batch 5b):  $\alpha$ -syn pSer129 level as fraction of total tissue area in ipsi- and contra-lateral brain regions. A, olfactory bulb (OB); B, anterior olfactory nucleus (AON); C, amygdala (AMY). See Methods and Fig. 1 for exposure paradigm and assays. \*,  $P < 0.05$ , \*\*,  $P < 0.01$ , \*\*\*,  $P < 0.0001$ , compared to PBS:N = 6-9.

### Gria1

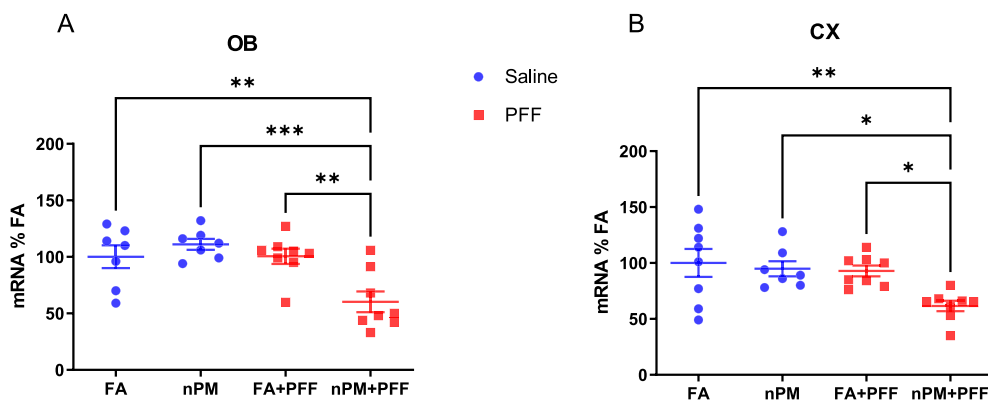


**Fig. 4.** Exposure 1, nPM Batch 5b: effect of PFF and nPM exposure on Gria1 mRNA in ipsilateral OB and frontal CX. A. OB, B. CX. \*,  $P < 0.05$ , \*\*,  $P < 0.01$ , \*\*\*,  $P < 0.001$ , N = 6-8.



Microglia cell density, assayed by Iba1 positive cells, did not differ in any region relative to control (Supplemental Fig. S1B-D). Similarly, the mRNAs of inflammatory cytokines *Tnfa*, *Il10* and the microglial marker *Cd68* did not differ from control (PBS + PFF) (Supplemental Fig. S2).

### 3.1.3. Effect on *Gria1* expression

In studies with prior batches of nPM, *Gria1* mRNA was downregulated [28,39,42,47]. In Exposure 1, *Gria1* mRNA did not respond to nPM Batch 5b in the ipsilateral OB ( $111 \pm 12.8$  for nPM vs  $100 \pm 26.6$  for FA,  $P = 0.93$ ,  $N = 8$ ) and frontal CX ( $94.9 \pm 17.9$  for nPM vs  $100 \pm 35.4$  for FA,  $P = 0.97$ ,  $N = 8$ ) (Fig. 4A and B). PFFs injection alone did not change *Gria1* mRNAs ( $100 \pm 18.9$ ,  $P = 0.99$ ,  $N = 8$  for OB and  $92.9 \pm 13.6$ ,  $P = 0.92$ ,  $N = 8$  for CX). However, the combination of PFFs and nPM (PFF + nPM) reduced *Gria1* mRNA in both ipsilateral OB ( $60.2 \pm 25.9$ ,  $P = 0.006$ ,  $N = 8$ ) and frontal CX ( $61.6 \pm 13.1$ ,  $P = 0.009$ ,  $N = 8$ ), compared with control (PBS + FA) (Fig. 4A and B).

## 3.2. Exposure 2 and 3: effect of PFFs injection during nPM exposure

Because of minimal response to nPM in Paradigm 1, we evaluated nPM exposure before PFF injection for interactive effects of  $\alpha$ -syn and with other nPM batches. At this time, we did not know that nPM batches had lower activity. Firstly, mice were exposed to nPM for 3 weeks, followed by PFF injections into the right OB, then with continued nPM exposure for another 7 weeks (Fig. 1, Exposure 2 and 3). Because of weak responses in Exposure 1, nPM exposure time was increased from 4-week to 7-week after injection of PFFs; animal number per group was also increased. Two nPM batches (Batch 7 and 9), which were subsequently found to have different toxicity [28], were used for Exposure 2 and 3, respectively. Batch 7 was the least active compared to other nPM batches collected at the same site but different dates, and Batch 9 was 3-times more active than Batch 7 as cited above.

### 3.2.1. Effect of nPM exposure on $\alpha$ -syn spread

We did not detect fibrillar  $\alpha$ -syn pSer129 in PBS-injected groups (data not shown), including both FA and nPM groups (for both Exposure 2 and 3). Seven weeks after PFF injection,  $\alpha$ -syn pSer129 was detected in ipsilateral OB, AON, AMY and piriform cortex (PCX), and significantly higher than that of the counterparts in the contralateral brain. For Exposure 2, ipsilateral  $\alpha$ -syn pSer129 was elevated by 9-, 6- and 9-fold in OB, AON and AMY, respectively; and for Exposure 3, it was elevated by 2-, 2- and 32-fold in OB, AON and PCX, respectively, above the contralateral, indicating the spread of  $\alpha$ -syn pSer129 pathology from the OB to ipsilateral regions (Fig. 5A-C, Exposure 2; 5D-F, Exposure 3). Consistent with Exposure 1 (Fig. 2), AON had the largest load of  $\alpha$ -syn pSer129 among ipsilateral regions (Exposure 2:  $2257 \pm 992$  in AON,  $78.2 \pm 44.5$  in OB, and  $42.1 \pm 25.3$  in AMY; Exposure 3:  $33.6 \pm 2.8$  in AON,  $4.4 \pm 1.6$  in OB, and  $15.6 \pm 2.2$  in PCX) (Fig. 5B and E). The absolute levels of  $\alpha$ -syn in Exposure 2 and Exposure 3 are not comparable due to different measurement methods.

No difference in  $\alpha$ -syn pSer129 levels in the ipsilateral OB (Exposure 2:  $78.2 \pm 44.5$  vs  $99.7 \pm 44.3$ ,  $p = 0.39$ ,  $n = 8$ ; Exposure 3:  $4.4 \pm 1.6$  vs  $4.0 \pm 2.1$ ,  $P = 0.61$ ,  $N = 10$ ), AON (Exposure 2:  $2257 \pm 997$  vs  $1780 \pm 557$ ,  $p = 0.26$ ,  $N = 8$ ; Exposure 3:  $33.6 \pm 2.8$  vs  $32.4 \pm 5.4$ ,  $P = 0.50$ ,  $N = 12$ ), AMY (Exposure 2:  $42.1 \pm 25.3$  vs  $59.8 \pm 34.7$ ,  $P = 0.27$ ,  $N = 8$ ) and PCX (Exposure 3:  $15.6 \pm 2.2$  vs  $15.5 \pm 4.1$ ,

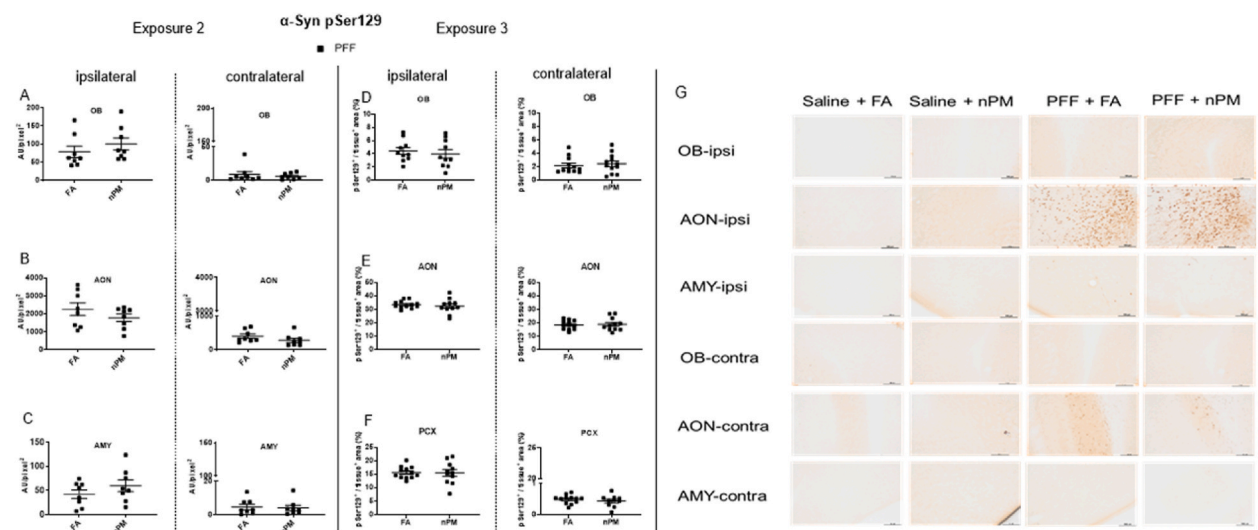


**Fig. 5.** Effect of nPM exposure on  $\alpha$ -syn pSer129 load in ipsi- or contra-lateral brain regions of Exposure 2 and 3. A, OB; B, AON; C, AMY for Exposure 2 (Batch 7). D, OB; E, AON; F, PCX for Exposure 3 (Batch 9); G, representative images of  $\alpha$ -syn pSer129 immunostaining in ipsi- and contra-lateral brain regions for Exposure 2, 20X images, scale bar, 100  $\mu$ m. Mice were exposed to nPM Batch 7 (Exposure 2) or Batch 9 (Exposure 3) for 3 weeks, then injected with PBS or PFF in right OB, followed by continued exposure to FA or nPM for 7 weeks. PBS injection groups had no  $\alpha$ -syn pSer129 signal; only results for PFF groups are shown.  $N = 8$ -10.

$P = 0.95$ ,  $N = 12$ ) was observed between FA and nPM groups injected with PFFs for both Exposure 2 and 3 (Fig. 5A–F); similarly the  $\alpha$ -syn pSer129 levels in the contralateral regions did not differ (Fig. 5A–F).

### 3.2.2. Microglial response

Iba1 expression in both ipsi- and contralateral OB and frontal CX did not differ between PFFs and the control (PBS + FA) group. In either the ipsi- or contra-lateral OB and CX, exposure to nPM Batches 7 and 9 alone, or its combination with PFFs, did not change Iba1 expression (Supplemental Fig. S4). Similarly, inflammatory cytokines or markers *Tnfa*, *Il1 $\beta$* , *Il10*, and *Cd68* in ipsi- and contra-lateral OB and frontal CX did not differ between experimental groups (PFF, nPM and nPM + PFF) and control (FA + PBS, Supplemental Fig. S4).

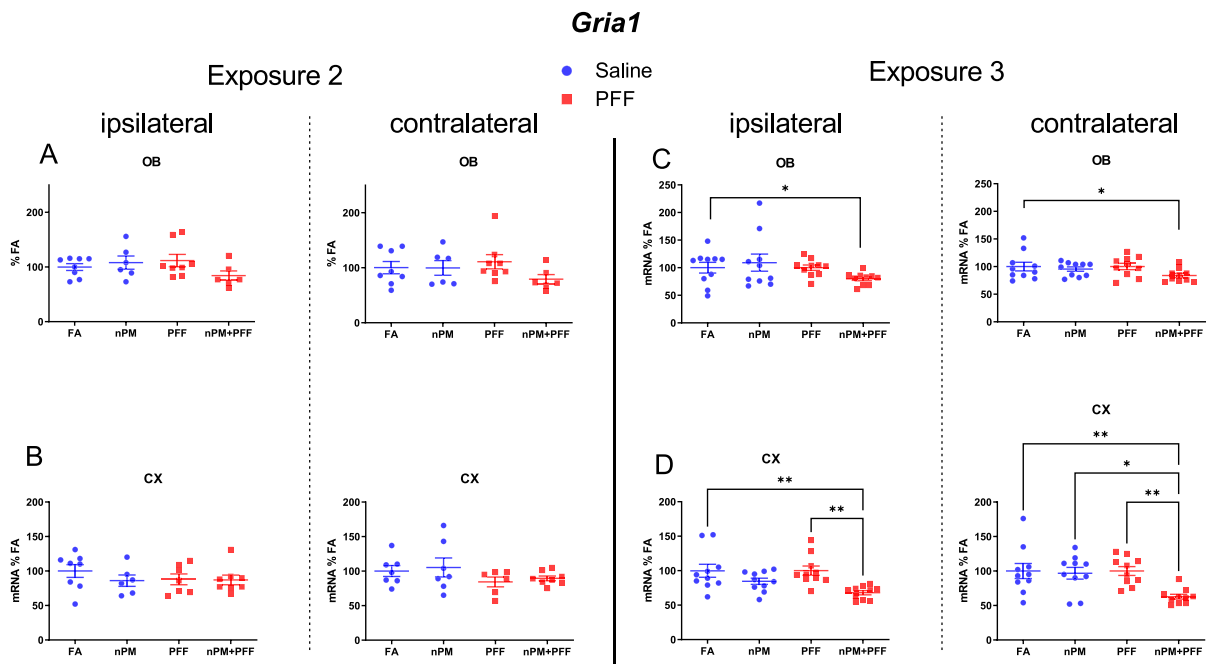
### 3.2.3. *Gria1* expression

Fig. 6 shows that for both Exposures 2 and 3, *Gria1* levels did not differ between control (PBS + FA) and PFF (PFF + FA) in both the ipsi- and contra-lateral OBs (Exposure 2-ipsi:  $99.9 \pm 17.9$  vs  $111 \pm 31.8$ ,  $P = 0.79$ ,  $N = 8$ ; Exposure 2-contra:  $100.1 \pm 28.5$  vs  $111 \pm 31.9$ ,  $P = 0.79$ ,  $N = 7$ ; Exposure 3-ipsi:  $100 \pm 30.4$  vs  $100 \pm 15.4$ ,  $P = 0.99$ ,  $N = 10$ ; Exposure 3-contra:  $100 \pm 24.9$  vs  $100 \pm 18.1$ ,  $P = 0.99$ ,  $N = 10$ ) (Fig. 6A, C) and frontal CX (Exposure 2-ipsi:  $100 \pm 26.2$  vs  $87.9 \pm 20.7$ ,  $P = 0.71$ ,  $N = 8$ ; Exposure 2-contra:  $100 \pm 20.8$  vs  $84.3 \pm 14.3$ ,  $P = 0.61$ ,  $N = 7$ ; Exposure 3-ipsi:  $99.8 \pm 22.7$  vs  $100 \pm 21.5$ ,  $P = 0.99$ ,  $N = 10$ ; Exposure 3-contra:  $100 \pm 34.4$  vs  $100 \pm 20.4$ ,  $P = 0.99$ ,  $N = 10$ ) (Fig. 6B, D), indicating  $\alpha$ -syn alone does not affect *Gria1* expression. Chronic exposure to nPM Batch 7 or Batch 9 also did not change *Gria1* expression in OB (Exposure 2-ipsi:  $108 \pm 29.7$  vs  $99.9 \pm 17.9$ ,  $P = 0.94$ ,  $N = 8$ ; Exposure 2-contra:  $108.4 \pm 37.6$  vs  $100 \pm 28.5$ ,  $P = 0.96$ ,  $N = 7$ ; Exposure 3-ipsi:  $100 \pm 30.4$  vs  $100 \pm 15.4$ ,  $P = 0.91$ ,  $N = 10$ ; Exposure 3-contra:  $95.5 \pm 12.6$  vs  $100 \pm 24.9$ ,  $P = 0.94$ ,  $N = 10$ ) (Fig. 6A, C) and frontal CX (Exposure 2-Ipsi:  $86.0 \pm 20.3$  vs  $100 \pm 26.2$ ,  $P = 0.65$ ,  $N = 8$ ; Exposure 2-contra:  $105 \pm 36.3$  vs  $100 \pm 20.8$ ,  $P = 0.97$ ,  $N = 7$ ; Exposure 3-ipsi:  $84.6 \pm 14.4$  vs  $99.8 \pm 22.7$ ,  $P = 0.35$ ,  $N = 10$ ; Exposure 3-contra:  $96.7 \pm 26.8$  vs  $100 \pm 34.4$ ,  $P = 0.99$ ,  $N = 10$ ) (Fig. 6B, D). Although combination of PFF and nPM Batch 7 did not alter *Gria1* expression, PFF and nPM Batch 9 together decreased *Gria1* mRNA by 20% and 16% in ipsi- and contralateral OB, respectively, and by 32% and 38% in ipsi- and contralateral frontal CX, respectively (Fig. 6C and D). The potency of nPM to down-regulate *Gria1* varied by nPM activities, e.g. Batch 9 was more active than Batch 7 in a prior study [28]. Overall, these results suggest that higher activity nPM batches interacted synergistically with  $\alpha$ -syn, leading to down-regulation of *Gria1*.

Statistical findings are summarized in Table 2.

## 4. Discussion

The population-based findings that air pollution exposure may increase risk for PD raises a major public concern, because most (>90%) of the world population lives in areas with chronically elevated air pollutants that exceed current US safety guidelines. However, experimental evidence linking air pollution and PD pathogenesis is incomplete. This study examined the impact of ambient



**Fig. 6.** Effect of nPM exposure and PFF on *Gria1* expression in ipsi- and contra-lateral OB and frontal CX. A, GluA1 protein in OB, immunohistochemistry; B, *Gria1* mRNA in frontal CX, qPCR; C and D, *Gria1* mRNA in OB and frontal CX for Exposure 3, qPCR. \*,  $P < 0.05$ , \*\*,  $P < 0.01$ ,  $N = 8-10$ .



**Table 2**  
Effects of nPM and PFF on  $\alpha$ -synuclein spread, microglial Iba1 and GluA1\*.

Exposure 1 (nPM Batch 5b)		OB	AON	AM	CX
Syn/ PFF	Ipsi > 14 fold; No nPM effect	Ipsi > 1000 fold; contra > 150 fold; No nPM effect	Ipsi > 200 fold; No nPM effect	N/A	
Iba1	No change	N/A	N/A	No change	
Gria1	Decreased by nPM + PFF, ipsi; contra N/A	N/A	N/A	Decreased by nPM + PFF, ipsi; contra N/A	
Exposure 2 (nPM Batch 7)		OB	AON	AM	CX
Syn/ PFF	Ipsi > 30 fold; No nPM effect	Ipsi > 10 fold; No nPM effect	Ipsi > 20 fold; No nPM effect	N/A	
Iba1	No change	N/A	N/A	No change	
Gria1	No effect	N/A	N/A	No effect	
Exposure 3 (nPM Batch 9)		OB	AON	AM	PCX or CX
Syn/ PFF	Ipsi > 2 fold; No nPM effect	Ipsi > 1.5 fold; No nPM effect	Ipsi > 10 fold; No nPM effect	N/A	
Iba1	No change	N/A	N/A	No change	
Gria1	Decreased by nPM + PFF, both sides	N/A	N/A	Decreased by nPM + PFF, both sides	

\* The effects/changes were compared with control (PBS + FA) group; N/A: not available.

nanoparticle exposure on the  $\alpha$ -syn propagation and its toxicity in an established mouse model of  $\alpha$ -syn propagation, triggered by injection of PFFs into the OB.

We used two experiment paradigms: in Paradigm 1, PFFs were injected before 4-week nPM exposure; and in Paradigm 2, PFFs were injected during 10-week nPM exposure. The nPM exposure caused a trend for increased  $\alpha$ -syn aggregation in Paradigm 1, but had no effect on  $\alpha$ -syn aggregation in Paradigm 2. In both paradigms, nPM and  $\alpha$ -syn synergistically down-regulated the expression of *Gria1* in the OB and frontal CX. After these studies were completed, these nPM batches collected at different dates were found to vary widely in toxicity [28,41]. These divergences in urban air pollution toxicity may explain why some previously published studies have not found strong associations between PD and air pollution [13].

$\alpha$ -Synuclein is a highly soluble, unfolded protein expressed throughout CNS. Misfolded  $\alpha$ -syn, either endogenously formed (e.g. PD) or exogenously introduced (e.g. intra-OB injection of PFFs), can seed the aggregation of natively unfolded  $\alpha$ -syn; the newly formed  $\alpha$ -syn fibrils are then potentially transported over long distances via axons and cause  $\alpha$ -syn aggregation in neurons that they have synaptic connections with [48]. This prion-like  $\alpha$ -syn propagation is believed to contribute to the spatial progression of PD pathology. Some environmental pollutants, such as rotenone [49] and paraquat [50], can cause the formation of Lewy body-like inclusions containing  $\alpha$ -syn and degeneration of the nigrostriatal dopaminergic pathway. In current experimental paradigms, exposure to ambient nPM alone for either 4 weeks (Paradigm 1) or 10 weeks (Paradigm 2) did not increase immunostaining for  $\alpha$ -syn pSer129, the predominant form of posttranslational modification of  $\alpha$ -syn in synucleinopathy [51], in any of the brain regions we studied (OB, AON, AMY and PCX), suggesting that nPM exposure does not trigger the formation of  $\alpha$ -Syn aggregates. Levesque et al. found that diesel exhaust particle exposure ( $\geq 311 \mu\text{g}/\text{m}^3$ ) for 6 months increased  $\alpha$ -syn (by 40–60%) in rat midbrain [20], however,  $\alpha$ -syn aggregation was not measured. We measured  $\alpha$ -syn pSer129 immunostaining but did not assay total  $\alpha$ -syn levels. As the elevation of  $\alpha$ -syn has been proposed a preclinical marker of PD [52], future study should measure if ambient nPM exposure influences total  $\alpha$ -syn levels, as opposed to just the pSer129 post-translationally modified form.

Consistent with the literature [29,30,33,34,53], intra-OB injection of  $\alpha$ -syn PFFs caused  $\alpha$ -syn propagation to other ipsilateral regions, including AON, PCX, and AMY (Figs. 2 and 4). In Paradigm 1, 4-week nPM exposure (Batch 5b) post the trigger of  $\alpha$ -syn pathology caused a trend for elevated  $\alpha$ -syn pSer129 in the ipsilateral OB, AON and AMY, and 43% increase in the overall load of  $\alpha$ -syn pSer129 in the ipsilateral regions (OB + AON + AMY); in contrast, in Paradigm 2, when  $\alpha$ -syn aggregation was triggered at 4th week during a 10-week-nPM exposure period,  $\alpha$ -syn pSer129 was not altered by nPMs (Batch 7 and 9). It is unclear whether the potential nPM effect on  $\alpha$ -syn aggregation in Paradigm 1 is due to longer post-injection time or different nPM activities: the  $\alpha$ -syn pSer129 was determined at different times after PFFs injection (15 weeks in Paradigm 1 vs 7 weeks in Paradigm 2) and different nPM batches were used.

Neuroinflammation is considered a pathogenic factor contributing to the development of  $\alpha$ -syn pathology [5,46,54]. Ambient nPM exposure can cause brain inflammation [39,40,42,55]. Thus, we hypothesized that nPM exposure could promote  $\alpha$ -syn propagation. Unexpectedly, none of the three nPM batches used in this study increased the expression of proinflammatory cytokines (Figs. S2 and S4) in OB and CX, or caused microglia activation in OB, AON and AMY (Supplemental Figs. S1 and S3). This may partially explain the weak effects of nPMs on  $\alpha$ -syn aggregation in these studies.

Misfolded  $\alpha$ -syn causes neuroinflammation and activate microglia in several PD models, including in  $\alpha$ -syn transgenic mice and in viral  $\alpha$ -syn overexpression mouse models [56–59]. In this study, however, the presence of  $\alpha$ -syn aggregates was not associated with microgliosis or inflammatory gene expression in the OB and CX at the time of analysis (Supplemental Figs. S1–S4). The weak inflammatory response to PFF injections is consistent with a report that inclusions of  $\alpha$ -syn did not increase Iba1-positive microglia in AON in the intra-OB PFF injection PD model [29]. Nonetheless, further studies are needed to evaluate how air pollution may influence  $\alpha$ -syn pathology in PD models where inflammation appears to play a central role at the outset.

Ambient particulate matters including nPM are a mixture and their components and toxic potency differ greatly depending on location and time of collection [28]. The *post hoc* comparisons of nPM Batches 7 and 9 with other nPM batches collected between 2016 and 2020 at the same site showed major variability for *in vitro* NF $\kappa$ B activation and oxidative stress response and *in vivo* neurotoxic responses [28]. Batch 9 causes stronger *in vitro* NF $\kappa$ B activation and *in vivo* brain responses than Batch 7, which exhibited the least activity among the previous ten nPM batches [28]; however, Batch 5b was not available to evaluate the relative activity. Despite their failure to induce microglial and cytokine responses, these nPM batches still caused some other brain responses. For instance, nPM Batch 9 did not induce pro-inflammatory cytokines, but it down-regulated *Nfkb1* and *Myd88* mRNAs in the brain [28]. Nonetheless, nPM batches used in current study are still representative of a real-world exposure, which varies widely by collection date at any location.

GluA1 is a postsynaptic membrane receptor mediating the glutamate signaling and synaptic function [37]; its deficiency leads to behavioral abnormalities, declined learning and memory, and impaired short-term olfaction memory [38,60–62]. *Gria1* expression did not decrease after exposure to any of the three nPM batches alone. However, when mice with  $\alpha$ -syn pathology were exposed to nPM Batch 5b and Batch 9, there was significant decrease of *Gria1* mRNA in the OB and frontal CX, bilaterally. This observation indicates a synergic interaction between nPM and  $\alpha$ -syn. Interestingly, the effect of  $\alpha$ -syn might be indirect as the degree of *Gria1* downregulation is similar in both hemispheres, despite that  $\alpha$ -syn pathology in the contra-lateral brain is much lower than in the ipsilateral. How this contributes to PD development—including its effects on non-motor symptoms like hyposmia and dementia, and on motor-symptoms, in which glutamate signaling plays an important role [63,64]—merits further study. Notably, *Gria1* was not decreased by the combination of  $\alpha$ -syn and nPM by Batch7, which had the least activity [28]. These data suggest that the adverse effects of air pollution exposure on PD pathology may vary with particle toxic potency, which in turn varies by location and season. This may explain the variable association of PD with air pollutants observed in population-based study [13].

Synergies with supra-additive effects are recognized between air pollution and other hazards or underlying health conditions. For example, Turner et al. reported that the joint effect of air pollution PM<sub>2.5</sub> and cigarette smoke on lung cancer mortality was stronger by 2.2 fold than their additive effect [65]. Similarly, Kim et al. reported that the combined exposure to both polycyclic aromatic hydrocarbon and second-hand smoke synergistically increased the risk of childhood obesity [66]. A recent study from our group also showed synergistic effects of nPM and chronic cerebral hypoperfusion on white matter injury in mice, by 2.3-fold above additive effects [59]—for this study, different nPM batches were used than the present experiments [28,67]. Mauderly et al. reviewed 36 laboratory studies on the combined effects of ozone and other pollutants (e.g. particles and cigarette smoke) on various endpoints that were reported in the U.S. Environmental Protection Agency Ozone Criteria Document, and found that 14 studies (39%) demonstrated synergism [68]. The underlying mechanism of this synergism remains unclear. Forman and Finch proposed that the crosstalk in detoxification pathways may potentially underlie the synergy between airborne particles and cigarette smoke [21]. Future research may define the mechanism of the synergy between airborne particle exposure and other environmental hazards or health conditions, including  $\alpha$ -syn pathology.

In summary, these experimental paradigms for exposure to ambient nPM did not have significant effects on  $\alpha$ -syn propagation and neuroinflammation; however, the data suggest that nPM and  $\alpha$ -syn can synergistically downregulate *Gria1* expression, depending upon nPM batch activity. The reduced expression of *Gria1* by combination of nPM and  $\alpha$ -syn suggests that air pollution may interact with  $\alpha$ -syn to affect PD pathogenesis. The variable activity of nPM batches available for these studies limits firm conclusions on how much air pollution may promote  $\alpha$ -synucleinopathy. Another limitation is that nPM lacks the polycyclic aromatic hydrocarbons (PAHs) in total ambient air pollution [69]. Future studies of PD and air pollution could consider using model particles, such as diesel exhaust particles (DEP) from the National Institute of Science and Technology (SRM 2975), which contain PAHs and can reliably induce neurotoxic responses as those caused by active nPM batches [70].

#### Author contribution statement

Hongqiao Zhang: Conceived and designed the experiments; Performed the experiments; Analyzed and interpreted the data; Wrote the paper.

Carla D'Agostino, Christopher Tulisiak, Liza Bergkvist, Lindsay Meyerdirk, Mafalda Cacciottolo: Performed the experiments; Analyzed and interpreted the data.

Max Andrew Thorwad, Allison Lindquist, Emily Schulz, Katelyn Becker, Mohit Kwatra, Jiyan Ma: Performed the experiments.

Jennifer A. Steiner: Analyzed and interpreted the data; Wrote the paper.

Nolwen L. Rey, Martha L. Escobar Galvis, Caleb E Finch, Patrik Brundin: Conceived the designed the experiments.

Constantinos Sioutas: Contributed reagents, materials, analysis tools and data.

#### Data availability statement

Data will be made available on request.

#### Declaration of interest's statement

The authors declare the following conflict of interests: Patrick Brundin has consulted for Axial Therapeutics, Calico, CuraSen, Enterin Inc, Fujifilm-Cellular Dynamics Inc, Idorsia and Lundbeck A/S. He has received commercial support for research from Lundbeck A/S and Roche, and has ownership interests in Acusort AB, Axial Therapeutics, Enterin Inc., Roche and RYNE

Biotechnology Inc. Patrick Brundin is currently an employee of F. Hoffman-La Roche. The other authors have no conflicts of interest to declare.

## Acknowledgements

This research was supported by grants from DoD Assistant Secretary of Defense for Health Affairs, Parkinson's Research Program Awards W81XWH-17-1-0535, Caleb E. Finch and W81XWH-17-1-0534, Patrik Brundin.

## Appendix A. Supplementary data

Supplementary data to this article can be found online at <https://doi.org/10.1016/j.heliyon.2023.e15622>.

## References

- [1] Y.C. Wong, D. Krainc, alpha-synuclein toxicity in neurodegeneration: mechanism and therapeutic strategies, *Nat. Med.* 23 (2017) 1–13.
- [2] N.L. Rey, D.W. Wesson, P. Brundin, The olfactory bulb as the entry site for prion-like propagation in neurodegenerative diseases, *Neurobiol. Dis.* 109 (2018) 226–248.
- [3] C.H. Hawkes, K. Del Tredici, H. Braak, Parkinson's disease: a dual-hit hypothesis, *Neuropathol. Appl. Neurobiol.* 33 (2007) 599–614.
- [4] E. Angot, J.A. Steiner, C. Hansen, J.Y. Li, P. Brundin, Are synucleinopathies prion-like disorders? *Lancet Neurol.* 9 (2010) 1128–1138.
- [5] M.G. Tansey, R.L. Wallings, M.C. Houser, M.K. Herrick, C.E. Keating, V. Joers, Inflammation and immune dysfunction in Parkinson disease, *Nat. Rev. Immunol.* 22 (2022) 657–673.
- [6] D. Chang, M.A. Nalls, I.B. Hallgrimsdottir, J. Hunkapiller, M. van der Brug, F. Cai, C. International Parkinson's Disease Genomics, T. andMe Research, G. A. Kerchner, G. Ayalon, B. Bingol, M. Sheng, D. Hinds, T.W. Behrens, A.B. Singleton, T.R. Bhangale, R.R. Graham, A meta-analysis of genome-wide association studies identifies 17 new Parkinson's disease risk loci, *Nat. Genet.* 49 (2017) 1511–1516.
- [7] N. Ball, W.P. Teo, S. Chandra, J. Chapman, Parkinson's disease and the environment, *Front. Neurol.* 10 (2019) 218.
- [8] S. Jo, Y.J. Kim, K.W. Park, Y.S. Hwang, S.H. Lee, B.J. Kim, S.J. Chung, Association of NO<sub>2</sub> and other air pollution exposures with the risk of Parkinson disease, *JAMA Neurol.* 78 (2021) 800–808.
- [9] C.Y. Chen, H.J. Hung, K.H. Chang, C.Y. Hsu, C.H. Muo, C.H. Tsai, T.N. Wu, Long-term exposure to air pollution and the incidence of Parkinson's disease: a nested case-control study, *PLoS One* 12 (2017).
- [10] E.F. Kirrane, C. Bowman, J.A. Davis, J.A. Hoppin, A. Blair, H.L. Chen, M.M. Patel, D.P. Sandler, C.M. Tanner, L. Vinikoor-Imler, M.H. Ward, T.J. Luben, F. Kamel, Associations of ozone and PM<sub>2.5</sub> concentrations with Parkinson's disease among participants in the agricultural health study, *J. Occup. Environ. Med.* 57 (2015) 509–517.
- [11] P.C. Lee, L.L. Liu, Y. Sun, Y.A. Chen, C.C. Liu, C.Y. Li, H.L. Yu, B. Ritz, Traffic-related air pollution increased the risk of Parkinson's disease in Taiwan: a nationwide study, *Environ. Int.* 96 (2016) 75–81.
- [12] P.C. Lee, O. Raaschou-Nielsen, C.M. Lill, L. Bertram, J.S. Sinsheimer, J. Hansen, B. Ritz, Gene-environment interactions linking air pollution and inflammation in Parkinson's disease, *Environ. Res.* 151 (2016) 713–720.
- [13] R. Liu, M.T. Young, J.C. Chen, J.D. Kaufman, H.L. Chen, Ambient air pollution exposures and risk of Parkinson disease, *Environ. Health Perspect.* 124 (2016) 1759–1765.
- [14] N. Palacios, K. Fitzgerald, J. Hart, M. Weisskopf, M. Schwarzschild, A. Ascherio, F. Laden, Air pollution and risk of Parkinson's disease in a large prospective study of men, *Neurology* 88 (2017).
- [15] B. Ritz, P.C. Lee, J. Hansen, C.F. Lassen, M. Ketzel, M. Sorensen, O. Raaschou-Nielsen, Traffic-Related air pollution and Parkinson's disease in Denmark: a case-control study, *Environ. Health Perspect.* 124 (2016) 351–356.
- [16] S. Shin, R.T. Burnett, J.C. Kwong, P. Hystad, A. van Donkelaar, J.R. Brook, R. Copes, K. Tu, M.S. Goldberg, P.J. Villeneuve, R.V. Martin, B.J. Murray, A.S. Wilton, A. Kopp, H. Chen, Effects of ambient air pollution on incident Parkinson's disease in Ontario, 2001 to 2013: a population-based cohort study, *Int. J. Epidemiol.* 47 (2018) 2038–2048.
- [17] W. Yuchi, H. Sbihi, H. Davies, L. Tamburic, M. Brauer, Road proximity, air pollution, noise, green space and neurologic disease incidence: a population-based cohort study, *Environ. Health* 19 (2020).
- [18] L. Calderon-Garciduenas, A. Gonzalez-Maciel, R. Reynoso-Robles, H.G. Silva-Pereyra, R. Torres-Jardon, R. Brito-Aguilar, A. Ayala, E.W. Stommel, R. Delgado-Chavez, Environmentally toxic solid nanoparticles in noradrenergic and dopaminergic nuclei and cerebellum of metropolitan Mexico city children and young adults with neural quadruple misfolded protein pathologies and high exposures to nano particulate matter, *Toxics* 10 (2022).
- [19] A. Haghani, T.E. Morgan, H.J. Forman, C.E. Finch, Air pollution neurotoxicity in the adult brain: emerging concepts from experimental findings, *J. Alzheimers Dis.* 76 (2020) 773–797.
- [20] S. Levesque, M.J. Surace, J. McDonald, M.L. Block, Air pollution & the brain: subchronic diesel exhaust exposure causes neuroinflammation and elevates early markers of neurodegenerative disease, *J. Neuroinflammation* 8 (2011).
- [21] H.J. Forman, C.E. Finch, A critical review of assays for hazardous components of air pollution, *Free Radic. Biol. Med.* 117 (2018) 202–217.
- [22] V.J. Farahani, A. Altuwayjiri, M. Pirhadi, V. Verma, A.A. Ruprecht, E. Diapouli, K. Eleftheriadis, C. Sioutas, The oxidative potential of particulate matter (PM) in different regions around the world and its relation to air pollution sources, *Environ. Sci.-Atmos.* 2 (2022) 1076–1086.
- [23] T. Xia, M. Kovichich, J. Brant, M. Hotze, J. Sempf, T. Oberley, C. Sioutas, J.I. Yeh, M.R. Wiesner, A.E. Nel, Comparison of the abilities of ambient and manufactured nanoparticles to induce cellular toxicity according to an oxidative stress paradigm, *Nano Lett.* 6 (2006) 1794–1807.
- [24] E. Vidrio, C.H. Phuah, A.M. Dillner, C. Anastasio, Generation of hydroxyl radicals from ambient fine particles in a surrogate lung fluid solution, *Environ. Sci. Technol.* 43 (2009) 922–927.
- [25] A. Saffari, N. Daher, M.M. Shafer, J.J. Schauer, C. Sioutas, Global perspective on the oxidative potential of airborne particulate matter: a synthesis of research findings, *Environ. Sci. Technol.* 48 (2014) 7576–7583.
- [26] C. Guastadisegni, F.J. Kelly, F.R. Cassee, M.E. Gerlofs-Nijland, N.A. Janssen, R. Pozzi, B. Brunekreef, T. Sandstrom, I. Mudway, Determinants of the proinflammatory action of ambient particulate matter in immortalized murine macrophages, *Environ. Health Perspect.* 118 (2010) 1728–1734.
- [27] X. Sun, H. Wei, D.E. Young, K.J. Bein, S.M. Smiley-Jewell, Q. Zhang, C.C.B. Fulgar, A.R. Castaneda, A.K. Pham, W. Li, K.E. Pinkerton, Differential pulmonary effects of wintertime California and China particulate matter in healthy young mice, *Toxicol. Lett.* 278 (2017) 1–8.
- [28] H. Zhang, C. D'Agostino, H.J. Forman, M. Cacciottolo, M. Thorwald, W.J. Mack, Q. Liu, K. Shkirkova, K. Lamorie-Foote, C. Sioutas, M. Pirhadi, W.J. Mack, T. E. Morgan, C.E. Finch, Urban air pollution nanoparticles from Los Angeles: recently decreased neurotoxicity, *J. Alzheimers Dis.* 82 (2021) 307–316.
- [29] N.L. Rey, J.A. Steiner, N. Maroof, K.C. Luk, Z. Madaj, J.Q. Trojanowski, V.M. Lee, P. Brundin, Widespread transneuronal propagation of alpha-synucleinopathy triggered in olfactory bulb mimics prodromal Parkinson's disease, *J. Exp. Med.* 213 (2016) 1759–1778.

- [30] N.L. Rey, S. George, J.A. Steiner, Z. Madaj, K.C. Luk, J.Q. Trojanowski, V.M. Lee, P. Brundin, Spread of aggregates after olfactory bulb injection of alpha-synuclein fibrils is associated with early neuronal loss and is reduced long term, *Acta Neuropathol.* 135 (2018) 65–83.
- [31] T.K. Kim, E.J. Bae, B.C. Jung, M. Choi, S.J. Shin, S.J. Park, J.T. Kim, M.K. Jung, A. Ulusoy, M.Y. Song, J.S. Lee, H.J. Lee, D.A. Di Monte, S.J. Lee, Inflammation promotes synucleinopathy propagation, *Exp. Mol. Med.* 54 (2022) 2148–2161.
- [32] S.A.M. Holec, J. Lee, A. Oehler, L. Batia, A. Wiggins-Gamble, J. Lau, F.K. Ooi, G.E. Merz, M. Wang, D.A. Mordes, S.H. Olson, A.L. Woerman, The E46K mutation modulates alpha-synuclein prion replication in transgenic mice, *PLoS Pathog.* 18 (2022), e1010956.
- [33] D.M. Mason, N. Nouraei, D.B. Pant, K.M. Miner, D.F. Hutchison, K.C. Luk, J.F. Stolz, R.K. Leak, Transmission of alpha-synucleinopathy from olfactory structures deep into the temporal lobe, *Mol. Neurodegener.* 11 (2016) 49.
- [34] D.M. Mason, Y. Wang, T.N. Bhatia, K.M. Miner, S.A. Trbojevic, J.F. Stolz, K.C. Luk, R.K. Leak, The center of olfactory bulb-seeded alpha-synucleinopathy is the limbic system and the ensuing pathology is higher in male than in female mice, *Brain Pathol.* 29 (2019) 741–770.
- [35] M.X. Henderson, E.J. Cornblath, A. Darwich, B. Zhang, H. Brown, R.J. Gathagan, R.M. Sandler, D.S. Bassett, J.Q. Trojanowski, V.M.Y. Lee, Spread of alpha-synuclein pathology through the brain connectome is modulated by selective vulnerability and predicted by network analysis, *Nat. Neurosci.* 22 (2019) 1248–1257.
- [36] M.X. Henderson, M. Sengupta, I. McGeary, B. Zhang, M.F. Olufemi, H. Brown, J.Q. Trojanowski, V.M.Y. Lee, LRRK2 inhibition does not impart protection from alpha-synuclein pathology and neuron death in non-transgenic mice, *Acta Neuropathol. Commun.* 7 (2019) 28.
- [37] S.F. Traynelis, L.P. Wollmuth, C.J. McBain, F.S. Menniti, K.M. Vance, K.K. Ogden, K.B. Hansen, H. Yuan, S.J. Myers, R. Dingledine, Glutamate receptor ion channels: structure, regulation, and function, *Pharmacol. Rev.* 62 (2010) 405–496.
- [38] G. Ang, L.A. Brown, S.K.E. Tam, K.E. Davies, R.G. Foster, P.J. Harrison, R. Sprengel, V.V. Vyazovskiy, P.L. Oliver, D.M. Bannerman, S.N. Peirson, Deletion of AMPA receptor GluA1 subunit gene (*Gria1*) causes circadian rhythm disruption and aberrant responses to environmental cues, *Transl. Psychiatry* 11 (2021) 588.
- [39] N.C. Woodward, P. Pakbin, A. Saffari, F. Shirmohammadi, A. Haghani, C. Sioutas, M. Cacciottolo, T.E. Morgan, C.E. Finch, Traffic-related air pollution impact on mouse brain accelerates myelin and neuritic aging changes with specificity for CA1 neurons, *Neurobiol. Aging* 53 (2017) 48–58.
- [40] H. Cheng, A. Saffari, C. Sioutas, H.J. Forman, T.E. Morgan, C.E. Finch, Nanoscale particulate matter from urban traffic rapidly induces oxidative stress and inflammation in olfactory epithelium with concomitant effects on brain, *Environ. Health Perspect.* 124 (2016) 1537–1546.
- [41] H. Zhang, A. Haghani, A.H. Mousavi, M. Cacciottolo, C. D'Agostino, N. Safi, M.H. Sowlat, C. Sioutas, T.E. Morgan, C.E. Finch, H.J. Forman, Cell-based assays that predict in vivo neurotoxicity of urban ambient nano-sized particulate matter, *Free Radic. Biol. Med.* 145 (2019) 33–41.
- [42] T.E. Morgan, D.A. Davis, N. Iwata, J.A. Tanner, D. Snyder, Z. Ning, W. Kam, Y.T. Hsu, J.W. Winkler, J.C. Chen, N.A. Petasis, M. Baudry, C. Sioutas, C.E. Finch, Glutamatergic neurons in rodent models respond to nanoscale particulate urban air pollutants in vivo and in vitro, *Environ. Health Perspect.* 119 (2011) 1003–1009.
- [43] J.D. Herner, P.G. Green, M.J. Kleeman, Measuring the trace elemental composition of size-resolved airborne particles, *Environ. Sci. Technol.* 40 (2006) 1925–1933.
- [44] E.A. Stone, C.J. Hedman, R.J. Sheesley, M.M. Shafer, J.J. Schauer, Investigating the chemical nature of humic-like substances (HULIS) in North American atmospheric aerosols by liquid chromatography tandem mass spectrometry, *Atmos. Environ.* 43 (2009) 4205–4213.
- [45] D. Chatterjee, D.S. Sanchez, E. Quansah, N.L. Rey, S. George, K. Becker, Z. Madaj, J.A. Steiner, J. Ma, M.L. Escobar Galvis, J.H. Kordower, P. Brundin, Loss of one *Engrailed1* allele enhances induced alpha-synucleinopathy, *J. Parkinsons Dis.* 9 (2019) 315–326.
- [46] S. George, N.L. Rey, T. Tyson, C. Esquibel, L. Meyerdirk, E. Schulz, S. Pierce, A.R. Burmeister, Z. Madaj, J.A. Steiner, M.L. Escobar Galvis, L. Brundin, P. Brundin, Microglia affect alpha-synuclein cell-to-cell transfer in a mouse model of Parkinson's disease, *Mol. Neurodegener.* 14 (2019) 34.
- [47] M. Cacciottolo, X. Wang, I. Driscoll, N. Woodward, A. Saffari, J. Reyes, M.L. Serre, W. Vizuete, C. Sioutas, T.E. Morgan, M. Gatz, H.C. Chui, S.A. Shumaker, S. M. Resnick, M.A. Espeland, C.E. Finch, J.C. Chen, Particulate air pollutants, APOE alleles and their contributions to cognitive impairment in older women and to amyloidogenesis in experimental models, *Transl. Psychiatry* 7 (2017), e1022.
- [48] S. George, N.L. Rey, N. Reichenbach, J.A. Steiner, P. Brundin, alpha-Synuclein: the long distance runner, *Brain Pathol.* 23 (2013) 350–357.
- [49] R. Betarbet, T.B. Sherer, G. MacKenzie, M. Garcia-Osuna, A.V. Panov, J.T. Greenamyre, Chronic systemic pesticide exposure reproduces features of Parkinson's disease, *Nat. Neurosci.* 3 (2000) 1301–1306.
- [50] A.B. Manning-Bog, A.L. McCormack, J. Li, V.N. Uversky, A.L. Fink, D.A. Di Monte, The herbicide paraquat causes up-regulation and aggregation of alpha-synuclein in mice: paraquat and alpha-synuclein, *J. Biol. Chem.* 277 (2002) 1641–1644.
- [51] H. Fujiwara, M. Hasegawa, N. Dohmae, A. Kawashima, E. Masliah, M.S. Goldberg, J. Shen, K. Takio, T. Iwatsubo, alpha-Synuclein is phosphorylated in synucleinopathy lesions, *Nat. Cell Biol.* 4 (2002) 160–164.
- [52] L.M. Chahine, M.B. Stern, Diagnostic markers for Parkinson's disease, *Curr. Opin. Neurol.* 24 (2011) 309–317.
- [53] T.N. Bhatia, R.N. Clark, P.G. Needham, K.M. Miner, A.S. Jamenis, E.A. Eckhoff, N. Abraham, X. Hu, P. Wipf, K.C. Luk, J.L. Brodsky, R.K. Leak, Heat shock protein 70 as a sex-skewed regulator of alpha-synucleinopathy, *Neurotherapeutics* 18 (2021) 2541–2564.
- [54] F. Blandini, Neural and immune mechanisms in the pathogenesis of Parkinson's disease, *J. Neuroimmune Pharmacol.* 8 (2013) 189–201.
- [55] R. Babadjouni, A. Patel, Q. Liu, K. Shkirkova, K. Lamorie-Foote, M. Connor, D.M. Hodis, H. Cheng, C. Sioutas, T.E. Morgan, C.E. Finch, W.J. Mack, Nanoparticulate matter exposure results in neuroinflammatory changes in the corpus callosum, *PLoS One* 13 (2018), e0206934.
- [56] W. Zhang, T. Wang, Z. Pei, D.S. Miller, X. Wu, M.L. Block, B. Wilson, W. Zhang, Y. Zhou, J.S. Hong, J. Zhang, Aggregated alpha-synuclein activates microglia: a process leading to disease progression in Parkinson's disease, *Faseb. J.* 19 (2005) 533–542.
- [57] A.D. Thome, A.S. Harms, L.A. Volpicelli-Daley, D.G. Standaert, microRNA-155 regulates alpha-synuclein-induced inflammatory responses in models of Parkinson disease, *J. Neurosci.* 36 (2016) 2383–2390.
- [58] C.P. Ramsey, M.G. Tansey, A survey from 2012 of evidence for the role of neuroinflammation in neurotoxin animal models of Parkinson's disease and potential molecular targets, *Exp. Neurol.* 256 (2014) 126–132.
- [59] H.E. Allen Reish, D.G. Standaert, Role of alpha-synuclein in inducing innate and adaptive immunity in Parkinson disease, *J. Parkinsons Dis.* 5 (2015) 1–19.
- [60] C. Barkus, M. Feyder, C. Graybeal, T. Wright, L. Wiedholz, A. Izquierdo, C. Kisilewicznyk, W. Schmitt, D.J. Sanderson, J.N. Rawlins, L.M. Saksida, T.J. Bussey, R. Sprengel, D. Bannerman, A. Holmes, Do GluA1 knockout mice exhibit behavioral abnormalities relevant to the negative or cognitive symptoms of schizophrenia and schizoaffective disorder? *Neuropharmacology* 62 (2012) 1263–1272.
- [61] D.J. Sanderson, S.B. McHugh, M.A. Good, R. Sprengel, P.H. Seeburg, J.N. Rawlins, D.M. Bannerman, Spatial working memory deficits in GluA1 AMPA receptor subunit knockout mice reflect impaired short-term habituation: evidence for Wagner's dual-process memory model, *Neuropsychologia* 48 (2010) 2303–2315.
- [62] K. Kilozzo, D. Strahnen, V. Prex, J. Gems, B. van der Veen, S.K.T. Kapanajah, B.K.B. Murthy, S. Schulz, R. Sprengel, D. Bannerman, D. Katzel, Distinct contributions of GluA1-containing AMPA receptors of different hippocampal subfields to salience processing, memory and impulse control, *Transl. Psychiatry* 12 (2022) 102.
- [63] Z. Zhang, S. Zhang, P. Fu, Z. Zhang, K. Lin, J.K. Ko, K.K. Yung, Roles of glutamate receptors in Parkinson's disease, *Int. J. Mol. Sci.* 20 (2019).
- [64] J. Wang, F. Wang, D. Mai, S. Qu, Molecular mechanisms of glutamate toxicity in Parkinson's disease, *Front. Neurosci.* 14 (2020), 585584.
- [65] M.C. Turner, A. Cohen, M. Jerrett, S.M. Gapstur, W.R. Diver, C.A. Pope 3rd, D. Krewski, B.S. Beckerman, J.M. Samet, Interactions between cigarette smoking and fine particulate matter in the risk of lung cancer mortality in cancer prevention study II, *Am. J. Epidemiol.* 180 (2014) 1145–1149.
- [66] H.W. Kim, S. Kam, D.H. Lee, Synergistic interaction between polycyclic aromatic hydrocarbons and environmental tobacco smoke on the risk of obesity in children and adolescents: the U.S. National Health and Nutrition Examination Survey 2003–2008, *Environ. Res.* 135 (2014) 354–360.
- [67] Q. Liu, K. Shkirkova, K. Lamorie-Foote, M. Connor, A. Patel, R. Babadjouni, M. Huuskonen, A. Montagne, H. Baertsch, H. Zhang, J.C. Chen, W.J. Mack, B. P. Walcott, B.V. Zlokovic, C. Sioutas, T.E. Morgan, C.E. Finch, W.J. Mack, Air pollution particulate matter exposure and chronic cerebral hypoperfusion and measures of white matter injury in a murine model, *Environ. Health Perspect.* 129 (2021), 87006.

- [68] J.L. Mauderly, J.M. Samet, Is there evidence for synergy among air pollutants in causing health effects? *Environ. Health Perspect.* 117 (2009) 1–6.
- [69] A. Haghani, R. Johnson, N. Safi, H. Zhang, M. Thorwald, A. Mousavi, N.C. Woodward, F. Shirmohammadi, V. Coussa, J.P. Wise Jr., H.J. Forman, C. Sioutas, H. Allayee, T.E. Morgan, C.E. Finch, Toxicity of urban air pollution particulate matter in developing and adult mouse brain: comparison of total and filter-eluted nanoparticles, *Environ. Int.* 136 (2020), 105510.
- [70] K. Shkirkova, K. Lamorie-Foote, N. Zhang, A. Li, A. Diaz, Q. Liu, M.A. Thorwald, J.A. Godoy-Lugo, B. Ge, C. D'Agostino, Z. Zhang, W.J. Mack, C. Sioutas, C. E. Finch, W.J. Mack, H. Zhang, Neurotoxicity of diesel exhaust particles, *J. Alzheimer's Dis.* 89 (2022) 1263–1278.